Journal of Materials Chemistry A

Accepted Manuscript

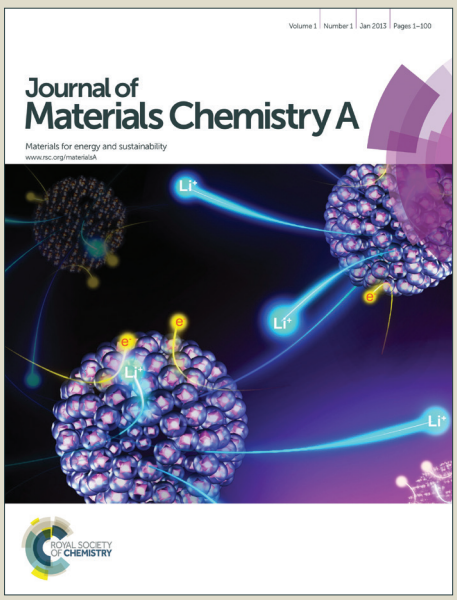

ROYAL SOCIETY OF CHEMISTRY

www.rsc.org/materialsA

Journal of Materials Chemistry A RSCPublishing

ARTICLE

Carbon-Coated Rhombohedral $Li_3V_2(PO_4)_3$ as Both Cathode and Anode Materials for Lithium-Ion Batteries: Electrochemical Performance and Lithium Storage Mechanism

Cite this: DOI: 10.1039/x0xx00000x

Received 00th January 2014,
Accepted 00th January 2014

DOI: 10.1039/x0xx00000x

www.rsc.org/

Zelang Jian,[a,†] Wenze Han,[b,†] Yanliang Liang,[a] Yucheng Lan,[c] Zheng Fang,[d] Yong-Sheng Hu[d] and Yan Yao[a,e*]

We report the electrochemical performance and storage mechanism of a symmetrical lithium ion battery made of carbon-coated rhombohedral $Li_3V_2(PO_4)_3$ (r-LVP/C) as both the cathode and anode materials. The electrochemical evaluation of r-LVP/C in lithium half-cells demonstrates reversible lithium extraction/insertion reactions at 3.75 V and average 1.75 V *vs.* Li^+/Li. Different storage mechanisms for the two reactions have been identified through *ex-situ* and *in-situ* X-ray diffraction measurements. A two-phase reaction takes place when two Li are extracted from r-LVP/C; while a solid-solution reaction happens when two Li are inserted into r-LVP/C. In comparison, only one Na ion can be inserted into its sodium counterpart, $Na_3V_2(PO_4)_3$. Symmetrical batteries presented a high capacity of 120 mAh/g with an operating voltage of ~ 2.0 V.

1. Introduction

In the last two decades, lithium-ion batteries (LIBs) have attracted significant attention because of the high energy/power density and broad application in consumer electronics and electric vehicles.[1-5] .

Polyanion-type $LiFePO_4$ has been used in power tools ad electric vehicles because of its stable structure and favorable electrochemical properties.[9-11] Other polyanion-type materials, such as $LiMPO_4$ (M = Mn, Co, Ni),[12-14] $Li_3M_2(PO_4)_3$ (M = V, Fe, Ti),[15-19] $Li_9M_3(PO_4)_2(P_2O_7)_3$ (M = V, Cr, Al, Ga)[20, 21] and $Li_2MP_2O_7$ (M = Mn, Co, Fe),[22, 23] have also been extensively investigated due to the great thermal stability and competitive energy density. Among these materials, $Li_3M_2(PO_4)_3$ (M = V, Fe, Ti) has attracted great attention due to its covalent three-dimensional structure with high ionic conductivity.[24-27] In particular, $Li_3V_2(PO_4)_3$ has been synthesized in two different forms: monoclinic $Li_3V_2(PO_4)_3$ (m-LVP) and rhombohedral $Li_3V_2(PO_4)_3$ (r-LVP).[19, 28, 29] m-LVP is the stable phase synthesized directly from high temperature solid-state reaction. The theoretical capacity is 131 mAh/g, corresponding to the extraction of two Li^+ ions. However, m-LVP exhibits multiple plateaus in the discharge curves at 4.1, 3.7, and 3.6 V. [30-32] In comparison, r-LVP shows more appealing discharge curves with the very flat plateau at 3.75 V vs. Li^+/Li, although it cannot be directly synthesized. Nazar *et al.* first reported the synthesis of r-LVP through a topotactic ion-exchange from r-$Na_3V_2(PO_4)_3$ in the concentrated $LiNO_3$ solution. 1.3 Li (corresponding to 85 mAh/g) were reported to be reversibly inserted back to the structure after the first 2-Li extraction.[28]

Rhombohedral NASICON structure with V^{4+}/V^{3+} redox couple have long been identified as candidates for high voltage cathode, [15, 28, 36] but there has been no report on using r-LVP as an anode material. In $Li_3V_2(PO_4)_3$, vanadium is at its intermediate valence state III, which can form two redox couples V^{4+}/V^{3+} and V^{3+}/V^{2+}. Li^+ ion not only can be extracted from the $Li_3V_2(PO_4)_3$ structure, but also can be further inserted into the structure. It has been reported that two additional Li can be inserted into the NASICON structure in the solid-solution fashion: $LiTi_2(PO_4)_3$[16] at average potential around 1.6V vs. Li^+/Li or $Li_3Fe_2(PO_4)_3$[17] at average potential around 2.75V vs. Li^+/Li. However, the sodium counterpart of r-LVP, can only

accommodate one additional Na at 1.63 V vs Na^+/Na.[37, 38] All these observations lead us to investigate the plausibility of exploring r-LVP as an anode material for lithium storage.

In this work, carbon-coated r-LVP (r-LVP/C) was obtained by ion-exchange method from r-NVP/C in a commercial electrolyte for LIBs. The carbon-coating strategy has been applied to various electrode materials to improve the electronic conductivity and protect the active materials.[33-35] We studied the structure of Li atomic site occupation in the r-LVP structure deduced from Rietveld-refined X-ray diffraction results. This material shows a flat plateau at 3.75 V *vs.* Li^+/Li and a slope with an average potential of 1.75 V *vs.* Li^+/Li. Excellent cycling and high-rate performance is observed when r-LVP/C is used as cathode. We report for the first time that two more Li can be inserted into the r-LVP structure, which is different from its sodium counterpart where only one Na could be inserted. We investigated the lithium storage mechanism of r-LVP/C by *in-situ* XRD and revealed a typical solid-solution reaction. Symmetrical batteries were also assembled and presented a high capacity of 120 mAh/g with an operating voltage of ~ 2.0 V.

2. Experimental Section

The carbon-coated rhombohedral $Na_3V_2(PO_4)_3$ compound (r-NVP/C) was synthesized by mixing a stoichiometric amount of NaH_2PO_4 (99.9%, Alfa Aesar), V_2O_3 (99.9%, Alfa Aesar) and glucose as carbon source. The mass ratio of V_2O_3 and glucose is 3.5:1, which means expected carbon content in the product is about 5%. The precursors were ball milled and then calcinated at 800 °C for 12 hours. The obtained r-NVP/C sample (1 g) was added to 1 M $LiPF_6$ in EC:DEC electrolyte (10 ml) and stirred overnight. The samples were centrifuged and washed with DI water for several times. The process was repeated twice to maximize the degree of ion exchange. The final sample was dried at 60 °C for 8 hours.

r-LVP/C was structurally characterized by XRD using a Bruker D8 Advance diffractometer using Cu Kα radiation (1.5405 Å). The morphology characterization was investigated using a scanning electron microscope (SEM, LEO Gemini 1525) and a transmission electron microscope (TEM, JEOL 2100F) operated at 200 keV. The carbon content was determined by thermogravimetric analysis (TGA).

A slurry containing 70 wt.% of r-LVP/C composite, 20 wt.% of carbon conductive additive and 10 wt.% of polyvinylidenefluofide (PVdF) was cast on an Al foil and dried in vacuum at 100 °C for 10 hours. The coin cells were assembled with Li metal as counter electrode with 1 M $LiPF_6$ EC:DEC (1:1) as electrolyte in an argon-filled glove box. The mass loading of the active materials was 2 mg/cm^2. Electrochemical measurements were performed using a LAND BT2000 battery cycler. For *in-situ* XRD measurements, an r-LVP/C electrode was used as a working electrode obtained by immersing an r-NVP/C electrode in 1M $LiPF_6$ in EC:DEC electrolyte. Polytetrafluoroethylene (PTFE) was used as the binder, and aluminium mesh was used as the current collector. Symmetrical cells were assembled by using r-LVP/C as active materials for both the cathode and the anode, where the mass ratio between cathode and anode is about 1:1.12. Discharge/charge tests were measured in the voltage range of 3.2–0 V.

3. Results and Discussion

The r-NVP/C sample was synthesized in a one-step solid-state reaction as reported in a previous study.[38] The r-LVP/C sample was prepared using a facile ion-exchange method (see experimental section). Inductively coupled plasma (ICP) was performed to identify the composition of the ion-exchange product. The result shows that the ratio of Li:Na:V is 2.832:0.168:1.991, corresponding to a composition of $Li_{2.83}Na_{0.17}V_2(PO_4)_3$, indicating nearly complete ion-exchange. Figure 1a shows that the XRD peak position and the relative intensity of the r-LVP/C sample are different from that of the r-NVP/C sample. The peaks of the r-LVP/C sample shift from low angles to high angles, and the strongest diffraction peak (113) shifts from 27.7° to 28.4°. Rietveld-refined XRD was conducted to further investigate the detailed structure of r-LVP; the results are shown in Figure 1b, and the crystal parameters are summarized in Table S1. The obtained parameters are reliable: R_p = 14.8; R_{wp} = 13.4; and R_{exp} = 9.1. All of the diffraction peaks of the r-LVP/C sample are indexed in a rhombohedral system with a space group of $R\bar{3}$ (Fig. 1a), which is different from the space group of $R\bar{3}C$ for r-NVP. The lattice constants of r-LVP (a = b = 8.329 Å, c = 22.518 Å) are determined from Rietveld-refined XRD. After the ion-exchange, the skeleton structure still remains and shares the corners of VO_6 octahedra and PO_4 tetrahedra. The *c* parameter of the unit cell slightly expands from 21.815 Å in r-NVP to 22.518 Å in r-LVP, which could be attributed to the strong electrostatic repulsion between VO_6 octahedra along the *c* axis after the Na^+ ion being replaced by the Li^+ ion.

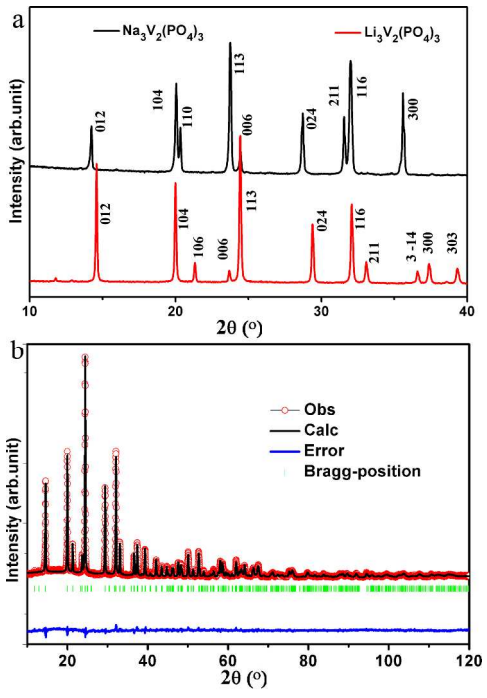

Figure 1. (a) XRD patterns of the r-NVP/C and r-LVP/C samples. (b) Rietveld-refined XRD results of the r-LVP/C sample, in which the observed data are indicated by black symbols and the calculated profile is represented by the red dotted line overlaying the black symbols. The residual discrepancy is shown in blue.

The schematic diagrams for the structure of r-LVP and r-NVP are shown in Figure 2. In the structure of r-LVP, the vanadium sites split into two distinct sites in the space group of $R\bar{3}$, resulting in two extra peaks at 11.7° and 12.9° in the powder diffraction pattern compared with the r-NVP structure (magnified XRD pattern in Figure S1). Phosphorus is still located at a single crystallographic site, forming PO_4 tetrahedra with oxygen. Li atoms fully occupy new crystallographic sites (18f), which are different from the original Na sites (6b and 18e), possibly due to the smaller ionic radii and (or) positional difference between Na^+ and Li^+.[39] The framework $[V_2(PO_4)_3]_\infty$ is parallel to the (a, b) plane where Li^+ ion layers are perpendicular to the *c* axis. The remaining Na^+ ions in the ion-exchanged r-LVP/C sample occupy 3a and 3b sites, which are equivalent to the 6b site in the r-NVP structure.

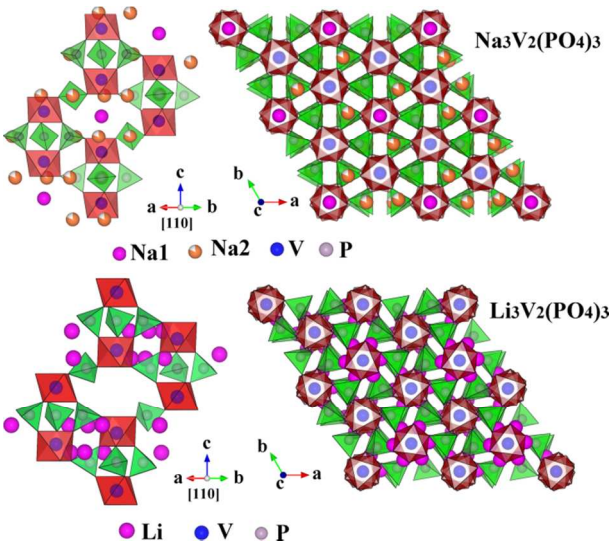

Figure 2. Schematic diagram of structure for $Na_3V_2(PO_4)_3$ (upper) and $Li_3V_2(PO_4)_3$ (lower).

SEM results (shown in Figure S3) show the similar morphology of the r-NVP/C and r-LVP/C samples. High-resolution transmission electron microscopy (HRTEM) was further carried out to investigate the r-NVP/C and r-LVP/C samples. After the ion-exchange, carbon still uniformly coats on the surface (Figure 3a and 3b); this result indicates that the ion-exchange method is successful. However, we could not observe the peak of carbon in the XRD pattern, indicating that carbon coating layer is amorphous, which is in good agreement with the TEM result. Figures 3c and 3d provide the lattice structures of the r-NVP/C and r-LVP/C samples. In the r-NVP/C sample, the lattice spacing of d = 0.38 nm corresponds to the (113) plane, which reflects the highest diffraction peak among XRD peaks. The lattice spacing in the r-LVP/C sample is d = 0.36 nm. The radius of Li^+ is much smaller than that of Na^+. When the Li^+ replaces the Na^+, the unit cell volume will shrink, leading to a reduced lattice spacing. The volume change from NVP to LVP is *ca.* 6%, which further proves the success of ion exchange. These results are consistent with the XRD data in that all diffraction peaks shift to higher angles. The carbon content of the two samples before and after ion-exchange was determined by TGA (Figure S2), which shows that the carbon content increases from 5.4% (carbon in r-NVP/C sample) to 6.6% (carbon in the r-LVP/C sample).

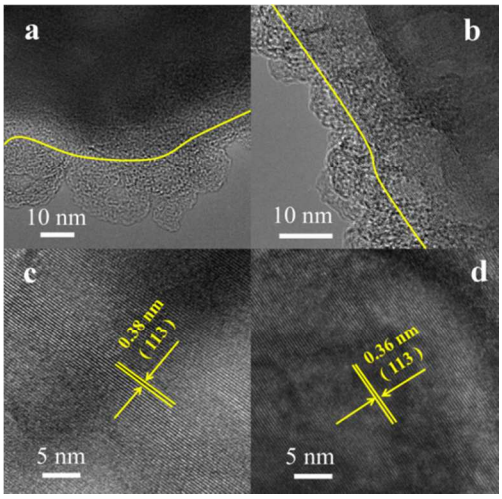

Figure 3. TEM images of the (a) r-NVP/C and (b) r-LVP/C samples. HR-TEM images of the (c) r-NVP/C and (d) r-LVP/C samples showing lattice information.

Figure 4a shows the cyclic voltammetry (CV) analysis of the r-LVP/C electrode at a scan rate of 0.05 mV/s in the voltage range of 3.0 V to 4.5 V *vs.* Li^+/Li. A pair of redox peaks is clearly observed at 3.64 and 3.89 V *vs.* Li^+/Li, higher than those of the r-NVP/C-Na cell for approximately 0.3 V because Li^+/Li exhibits a lower redox voltage than that of Na^+/Na. Since no other peak could be observed from the CV curves, the pair of redox peaks should correspond to the V^{3+}/V^{4+} redox couple. In the first cycle, the redox peaks are slightly broader than those in the following cycles, which is probably due to the presence of residual Na^+ ions that have not been ion-exchanged completely. The subsequent CV curves almost overlap, indicating an excellent cycling performance. Figure 4b shows the charge/discharge curves of the r-LVP/C electrode during the first five cycles, 20th cycle and 40th cycle at a rate of 0.1C. There is a very flat plateau at 3.75 V *vs.* Li^+/Li, which is consistent with the CV result. The r-LVP/C sample delivers an initial charge capacity of 120 mAh/g and a high reversible discharge capacity of 113 mAh/g. Taking the presence of 6.6% carbon in the r-LVP/C sample into account, the observed capacity (121 mAh/g) is very close to the theoretical value (131 mAh/g) of the two Li insertion. The reason that only two-thirds of the Li ions could be extracted out from the structure is because once two-thirds of Li ions were extracted from the tetrahedral sites, the remaining one-third of Li ions will diffuse to 3a or 3b site and could not been further extracted.[18] Figure 4c shows the cycling performance. After 40 cycles, reversible capacity could be maintained at 108 mAh/g, which is 96% of the original reversible

capacity. The initial coulombic efficiency is 94.2% and increases to 99% in later cycles. The magnified flat regions of the charge/discharge curves are shown in Figure 4d. The voltage hysteresis of only ~ 40 mV is very small and does not increase during the 40 cycles, indicating excellent electronic and ionic conductivity and great stability. Overall the r-LVP/C sample shows excellent electrochemical performance.

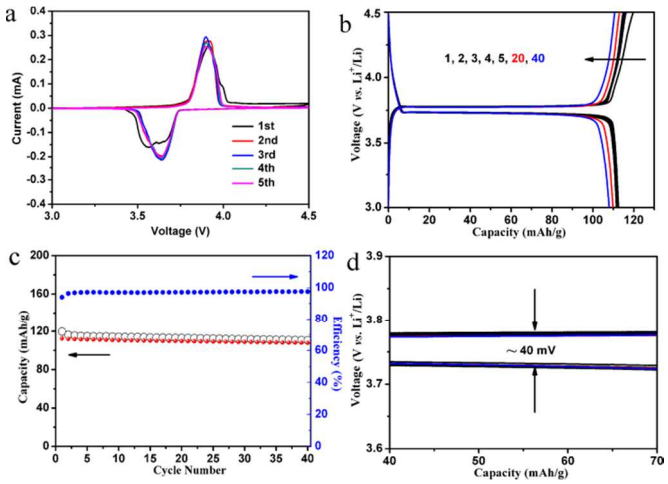

Figure 4. (a) CV curves of the r-LVP/C electrode in a voltage range of 3.0 V to 4.5 V at a scan rate of 0.05 mV/s; (b) selected charge/discharge curves of the r-LVP/C electrode at a rate of 0.1C; (c) cycling performance of the r-LVP/C electrode at 0.1C; and (d) the magnified flat region of the charge/discharge curves.

We investigated the rate capability of the r-LVP/C sample and compared it with that of the r-NVP/C sample. Figure 5a shows that the r-LVP/C electrode generally exhibits a higher capacity than that of its sodium counterpart, particularly at high rates (2C and 5C). r-LVP has a large theoretical capacity (131 mAh/g) than that of r-NVP (117 mAh/g). Therefore, the difference at low rates in capacity is small because both samples can approach their theoretical capacity. At higher rates, r-LVP/C shows the reversible capacity of 97.7 and 76 mAh/g at 2C and 5C, respectively. In comparison, r-NVP/C shows the reversible capacity of only 57 and 8 mAh/g. This difference in the rate performance is mainly due to the smaller ionic radius of Li^+ than that of Na^+.

The charge/discharge voltage profiles at different C-rates are shown in Figure 5b. The reversible capacities are 111.4, 110.6, 108.2, 103.8, 97.7 and 76 mAh/g at 0.1C, 0.2C, 0.5C, 1C, 2C and 5C, respectively. Its capacity remains almost unchanged at low rates. Even at 2C and 5C, the capacity remains at approximately 87.7% and 68.2% of the original capacity (0.1 C), respectively. Furthermore, voltage hysteresis slightly increases with the C-rate increasing. Even at 2C, its overvoltage is only ~240 mV. The excellent C-rate performance of the r-LVP/C sample could be attributed to the uniform carbon coating and the inherently high ionic conductivity of the NASICON structure. The long cycling performance is shown in Figure 5c. After 300 cycles at 1C, capacity is still higher than 90 mAh/g and shows high coulombic efficiency of ~99%. A good long cycling performance is attributed to the uniform carbon coating and minimum volume change during charge/discharge. The carbon coating layer can prevent r-LVP from directly interacting with electrolytes, thereby inhibiting any side reaction.

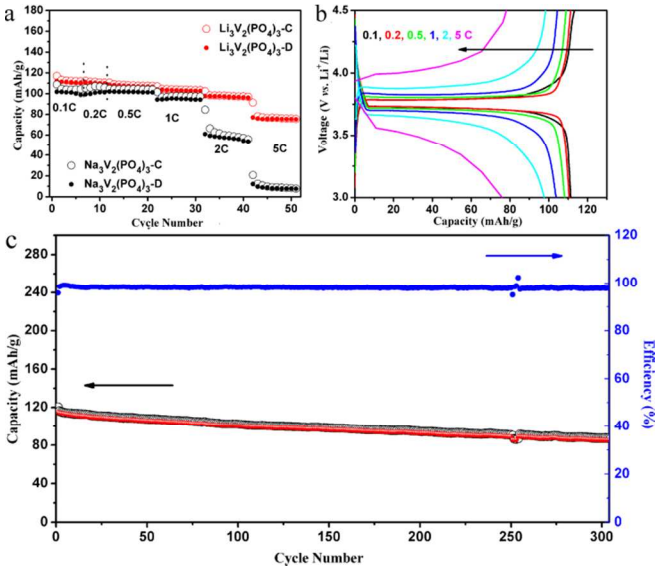

Figure 5. (a) Rate performance of r-LVP/C and r-NVP/C; (b) Typical charge/discharge curves of the r-LVP/C electrode at different C-rates; 1 C refers to the two Li extraction from r-LVP per formula unit in 1 hour. (c) 300 cycles of r-LVP/C at 1C with 77% capacity retention.

Ex-situ XRD is conducted to understand the lithium storage mechanism of r-LVP. Figure 6 shows the XRD patterns of the r-LVP/C electrode with various state-of-charge (Figure 6a): pristine (A), half-charged (B), fully-charged (C), half-discharged (D) and fully-discharged (E). Peaks of the aluminum substrate are observed near the 28.5° and 44.7°. New diffraction peaks, such as 21°, 24.7°, 29.9°, 32.6° and 33.7° (marked by blue ♥), are observed when an electrode is in a half-charged state. The new diffraction peaks shift from low angles to high angles (C), corresponding to a decrease in the crystalline interplanar spacing that resulted from the Li extraction. Considering the electrochemical result, we conclude that the new diffraction peaks belong to rhombohedral $LiV_2(PO_4)_3$. Two phases also co-exist in the 50% discharged state (D). All diffraction peaks revert to those of the r-LVP structure when an electrode is fully discharged (E). *Ex-situ* XRD results indicate that the mechanism of lithium storage in r-LVP is a typical two-phase reaction, which is similar to that of its sodium counterpart. However, the volume change of approximately 6.11% is considered small,[25] even smaller than that of $LiFePO_4$ (6.81%)[9]. The completely reversible structural evolution in the charge/discharge process is closely related to the stable cycling of the r-LVP/C sample.

As is known, r-NVP/C[38] and m-LVP[40] can also be used as anode for sodium-ion batteries. Only one Na can be inserted into the r-NVP structure[38] and two Li can insert into m-LVP structure[40]. Here, we investigated the Li insertion capability of the r-LVP/C. The discharge/charge curves in the voltage range of 3.0–1.0 V *vs.* Li^+/Li

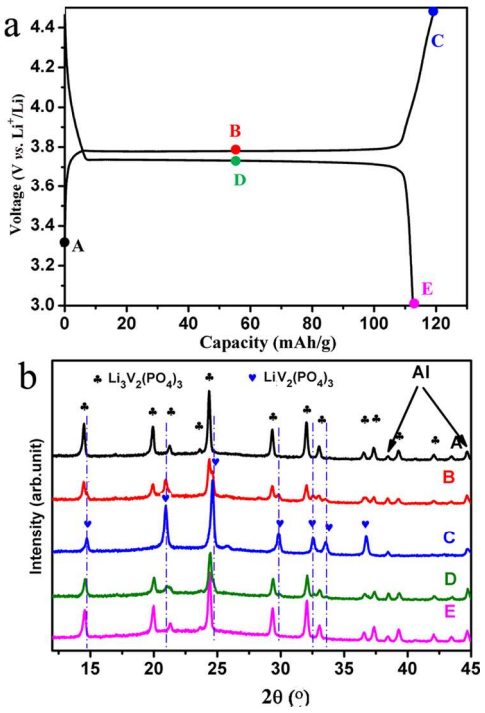

Figure 6. *Ex-situ* XRD patterns (b) of the r-LVP/C electrode at various state-of-charge indicated in the voltage profile (a).

are shown in Figure 7a. The initial discharge/charge capacity is 136/117 mAh/g at a rate of 0.1C, which corresponds to two Li insertion into the r-LVP structure. Its subsequent discharge/charge curves are almost overlapped, indicating good cycling performance. The long cycling performance at a rate of 1 C is shown in Figure 7b, which shows initial reversible capacity of 98.3 mAh/g. The subsequent coulombic efficiency is close to 100% and the capacity retention is 76% over 500 cycles.

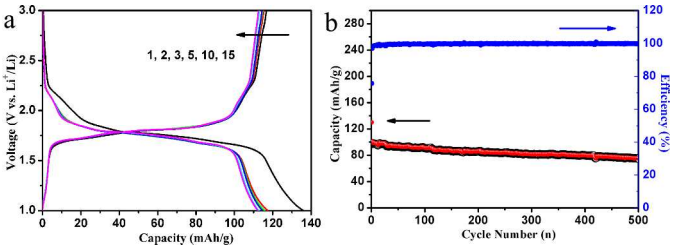

Figure 7. (a) Selected discharge/charge curves of the r-LVP/C electrode at a rate of 0.1C in the voltage range of 3.0–1.0 V *vs.* Li^+/Li; (b) 500 cycles of r-LVP/C at 1C with 76% capacity retention.

Furthermore, we find that discharge/charge curves show a sloping profile with average voltage of 1.75 V *vs.* Li^+/Li, which is very different from the discharge/charge curves of the r-NVP/Na cell (Figure S4), indicating a different storage mechanism. Five Li can be accommodated in the r-LVP structure while only four Na can be accommodated in the r-NVP structure. These can be ascribed to the difference in space groups of r-LVP and r-NVP and ion radii of lithium and sodium. Two additionally inserted Li atoms will occupy 3a (0.5 Li), 3b (0.5 Li) and 6c (1 Li) with the schematic diagram shown in Figure 8a. Figure 8b exhibits the *in-situ* XRD result of r-LVP/C during the discharge and charge process. We observed continuous shift of diffraction peaks to the lower angles when Li was inserted during the discharge process, and peaks shift to the higher angles when Li was extracted during the charge process. This result indicates a typical solid-solution reaction.

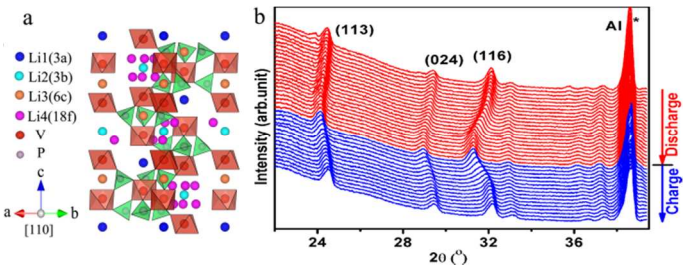

Figure 8. (a) Possible structure of r-LVP after two more Li insertion at [110] orientation; (b) *in-situ* XRD patterns of the r-LVP/C-Li battery cycled at the voltage of 3.0 and 1.0 V *vs.* Li^+/Li at a rate of 0.1C.

Since r-LVP/C can be oxidized (two Li extraction) at 3.75 V *vs.* Li^+/Li and be reduced (two Li insertion) at an average potential of 1.75 V *vs.* Li^+/Li, respectively, this material could be assembled into a symmetrical full cell, i.e. r-LVP/C was used as both the cathode and the anode. Figure 9 shows that the full cell delivers an average operating voltage of about 2.0 V, which is in good agreement with the theoretical output voltage. The reversible capacity can reach 120 mAh/g (based on the weight of cathode material). The energy density of the symmetrical full cell based on the total mass of cathode and anode (in a 1:1.12 ratio) is 113 Wh/kg, which can be potentially used for large-scale energy storage. Further optimization for the symmetrical full cell is in progress.

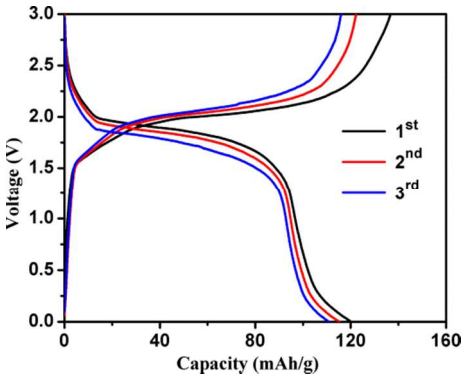

Figure 9. The charge/discharge profiles for the symmetrical full cell in $LiPF_6$/EC+DEC electrolyte at a current rate of 0.1C in a voltage range of 3.2–0 V (the capacity is calculated based on the mass of cathode. The capacity ratio of cathode:anode is 1:1.12.).

4. Conclusions

In summary, carbon-coated r-LVP samples were synthesized by the ion-exchange method. After the ion-

exchange, the structure evolved from the $R\bar{3}C$ group to the $R\bar{3}$ group. All Li atoms occupy the same sites (18f) in the r-LVP structure. The r-LVP/C sample shows a flat plateau at 3.75 V *vs.* Li^+/Li with a very small overpotential (~ 40 mV) and a slope with the average voltage at 1.75 V *vs.* Li^+/Li. When used as a cathode, r-LVP/C exhibits excellent rate and long cycling performance. At 2C and 5C, the reversible capacity can reach 97.7 and 76 mAh/g, respectively. The capacity remains at 90 mAh/g after 300 cycles at a rate of 1C. *Ex-situ* XRD results indicate that the lithium storage mechanism is a typical two-phase reaction with a small volume change of 6.11%. The reversible structural change during the charge/discharge process contributes to the excellent electrochemical performance of the r-LVP/C sample. Further study indicates that the r-LVP/C sample can also be used as an anode for LIBs, which delivers a reversible capacity of 117 mAh/g (two Li insertion). Its capacity retention rate is 76% over 500 cycles at 1C. These excellent properties make r-LVP both promising cathode and anode candidates for LIBs. A symmetrical full cell exhibits a reversible capacity of 120 mAh/g with an operating voltage of ~2.0 V.

Acknowledgements

Y. Y. acknowledges the support from National Science Foundation (CMMI-1400261), Robert A. Welch Professorship at TcSUH (E-0001). Y. Hu acknowledges "973" Project (2012CB932900, China) and NSFC (No. 11205249, China).

Notes and references

[a] Department of Electrical and Computer Engineering, University of Houston, Houston, Texas 77204, USA.
E-mail: yyao4@uh.edu
[b] China Institute of Atomic Energy, Beijing 102413, China.
[c] Department of Physics, University of Houston, Houston, Texas 77204, USA
[d] Beijing National Laboratory for Condensed Matter Physics, Institute of Physics, Chinese Academy of Science, Beijing 100190, China
[e] Texas Center for Superconductivity at the University of Houston, Houston, Texas 77204, USA
† Z. L. Jian and W. Z. Han contributed equally to this work.
Electronic Supplementary Information (ESI) available: Crystallographic data of the r-LVP/C; magnified XRD pattern of r-LVP/C; TG curves of r-NVP/C and r-LVP/C; SEM images of r-NVP/C and r-LVP/C; typical discharge/charge of r-NVP/C as anode. See DOI: 10.1039/b000000x/

1. M. Armand and J.-M. Tarascon, *Nature*, 2008, **451**, 652-657.
2. H. Li, Z. Wang, L. Chen and X. Huang, *Advanced Materials*, 2009, **21**, 4593-4607.
3. B. Kang and G. Ceder, *Nature*, 2009, **458**, 190-193.
4. M. S. Whittingham, *Mrs Bulletin*, 2008, **33**, 411-419.
5. R. Van Noorden, *Nature*, 2014, **507**, 26-28.
6. M. S. Whittingham and T. Zawodzinski, *Chemical reviews*, 2004, **104**, 4243-4244.
7. D. J. Klionsky, F. C. Abdalla, H. Abeliovich, R. T. Abraham, A. Acevedo-Arozena, K. Adeli, L. Agholme, M. Agnello, P. Agostinis and J. A. Aguirre-Ghiso, *Autophagy*, 2012, **8**, 445-544.
8. Y. G. Guo, J. S. Hu and L. J. Wan, *Advanced Materials*, 2008, **20**, 2878-2887.
9. A. K. Padhi, K. Nanjundaswamy and J. B. d. Goodenough, *Journal of the Electrochemical Society*, 1997, **144**, 1188-1194.
10. Y. Wang, Y. Wang, E. Hosono, K. Wang and H. Zhou, *Angewandte Chemie*, 2008, **120**, 7571-7575.
11. A. Yamada, S.-C. Chung and K. Hinokuma, *Journal of the Electrochemical Society*, 2001, **148**, A224-A229.
12. D. Choi, D. Wang, I.-T. Bae, J. Xiao, Z. Nie, W. Wang, V. V. Viswanathan, Y. J. Lee, J.-G. Zhang and G. L. Graff, *Nano letters*, 2010, **10**, 2799-2805.
13. C. Delacourt, L. Laffont, R. Bouchet, C. Wurm, J.-B. Leriche, M. Morcrette, J.-M. Tarascon and C. Masquelier, *Journal of the Electrochemical Society*, 2005, **152**, A913-A921.
14. V. Aravindan, J. Gnanaraj, Y.-S. Lee and S. Madhavi, *Journal of Materials Chemistry A*, 2013, **1**, 3518-3539.
15. Q. Wei, Q. An, D. Chen, L. Mai, S. Chen, Y. Zhao, K. M. Hercule, L. Xu, A. Minhas-Khan and Q. Zhang, *Nano letters*, 2014, **14**, 1042-1048.
16. C. Delmas, A. Nadiri and J. L. Soubeyroux, *Solid State Ionics*, 1988, **28**, 419-423.
17. C. Masquelier, A. Padhi, K. Nanjundaswamy and J. Goodenough, *Journal of Solid State Chemistry*, 1998, **135**, 228-234.
18. S.-C. Yin, H. Grondey, P. Strobel, M. Anne and L. Nazar, *Journal of the American Chemical Society*, 2003, **125**, 10402-10411.
19. H. Huang, S. C. Yin, T. Kerr, N. Taylor and L. F. Nazar, *Advanced Materials*, 2002, **14**, 1525-1528.
20. G. Ceder, A. Jain, G. Hautier, J. C. Kim, B. Kang and R. Daniel, Google Patents, 2013.
21. A. Jain, G. Hautier, C. Moore, B. Kang, J. Lee, H. Chen, N. Twu and G. Ceder, *Journal of the Electrochemical Society*, 2012, **159**, A622-A633.
22. P. Barpanda, T. Ye, S.-C. Chung, Y. Yamada, S.-i. Nishimura and A. Yamada, *Journal of Materials Chemistry*, 2012, **22**, 13455-13459.
23. M. Tamaru, P. Barpanda, Y. Yamada, S.-i. Nishimura and A. Yamada, *Journal of Materials Chemistry*, 2012, **22**, 24526-24529.
24. H.-P. Hong, *Materials Research Bulletin*, 1978, **13**, 117-124.
25. V. Thangadurai and W. Weppner, *Ionics*, 2002, **8**, 281-292.
26. J. Shi, G. Yin, L. Jing, J. Guan, M. Wu, Y. Zhou, H. Lou and Z. Wang, *International Journal of Modern Physics B*, 2014, **28**, 1450176.
27. D. Han, S.-J. Lim, Y.-I. Kim, S. H. Kang, Y. C. Lee and Y.-M. Kang, *Chemistry of Materials*, 2014, **26**, 3644–3650.
28. J. Gaubicher, C. Wurm, G. Goward, C. Masquelier and L. Nazar, *Chemistry of materials*, 2000, **12**, 3240-3242.
29. Y. Lu, L. Wang, J. Song, D. Zhang, M. Xu and J. B. Goodenough, *Journal of Materials Chemistry A*, 2013, **1**, 68-72.
30. M. Ren, Z. Zhou, X. Gao, W. Peng and J. Wei, *The Journal of Physical Chemistry C*, 2008, **112**, 5689-5693.
31. Y. Luo, X. Xu, Y. Zhang, Y. Pi, Y. Zhao, X. Tian, Q. An, Q. Wei and L. Mai, *Advanced Energy Materials*, 2014, DOI: 10.1002/aenm.201400107.

32. J. Xu, S.-L. Chou, C. Zhou, Q.-F. Gu, H.-K. Liu and S.-X. Dou, *Journal of Power Sources*, 2014, **246**, 124-131.
33. J. Wang and X. Sun, *Energy & Environmental Science*, 2012, **5**, 5163-5185.
34. G.-N. Zhu, H.-J. Liu, J.-H. Zhuang, C.-X. Wang, Y.-G. Wang and Y.-Y. Xia, *Energy & Environmental Science*, 2011, **4**, 4016-4022.
35. Z. Jian, L. Zhao, R. Wang, Y.-S. Hu, H. Li, W. Chen and L. Chen, *RSC Adv.*, 2012, **2**, 1751-1754.
36. B. L. Cushing and J. B. Goodenough, *Journal of Solid State Chemistry*, 2001, **162**, 176-181.
37. S. Li, Y. Dong, L. Xu, X. Xu, L. He and L. Mai, *Advanced Materials*, 2014, **26**, 3358-3358.
38. Z. Jian, L. Zhao, H. Pan, Y.-S. Hu, H. Li, W. Chen and L. Chen, *Electrochemistry Communications*, 2012, **14**, 86-89.
39. Z. Jian, C. Yuan, W. Han, X. Lu, L. Gu, X. Xi, Y. S. Hu, H. Li, W. Chen and D. Chen, *Advanced Functional Materials*, 2014, **24**, 4265–4272.
40 A. S. Hameed, M.V. Reddy, B.V.R. Chowdari, J. J. Vittala, Electrochim. Acta, 2014, **128**, 184-191.

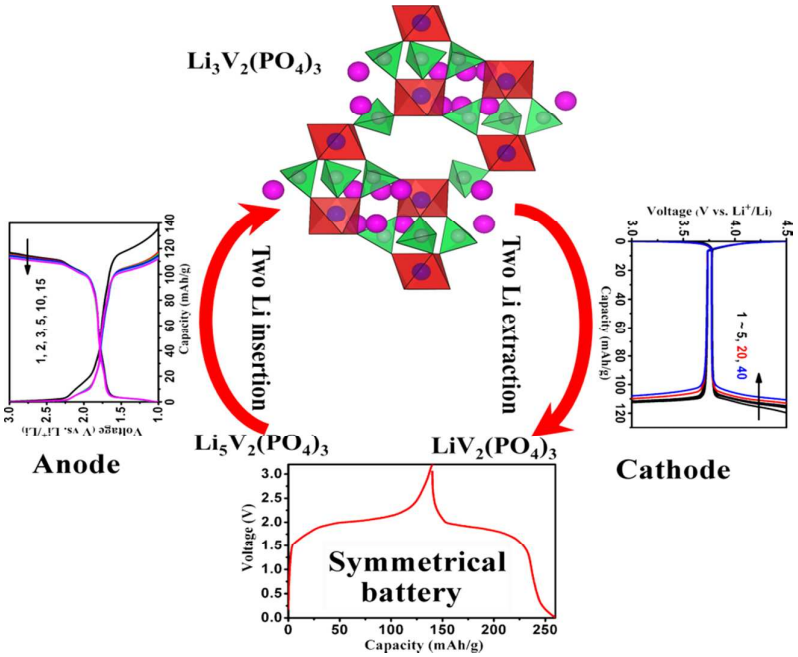

We report the electrochemical performance and storage mechanism of a symmetrical lithium ion cell made of carbon-coated rhombohedral $Li_3V_2(PO_4)_3$.